International Journal of Pharmaceutics 419 (2011) 85–95

Contents lists available at ScienceDirect

International Journal of Pharmaceutics

journal homepage: www.elsevier.com/locate/ijpharm

Liposome formulated with TAT-modified cholesterol for enhancing the brain delivery

Yao Qin[a,c], Huali Chen[a], Wenmin Yuan[a], Rui Kuai[a], Qianyu Zhang[a], Fulan Xie[a], Li Zhang[a], Zhirong Zhang[a], Ji Liu[b,*], Qin He[a,**]

[a] Key Laboratory of Drug Targeting and Drug Delivery Systems, West China School of Pharmacy, Sichuan University, No. 17, Block 3, Southern Renmin Road, Chengdu 610041, Sichuan, PR China
[b] West China School of Preclinical and Forensic Medicine, Sichuan University, No. 17, Block 3, Southern Renmin Road, Chengdu 610041, Sichuan, PR China
[c] Taiji Group, No. 38, Huanglong Road, Chongqing 401147, PR China

ARTICLE INFO

Article history:
Received 18 May 2011
Received in revised form 27 June 2011
Accepted 14 July 2011
Available online 23 July 2011

Keywords:
TAT
Cholesterol
Liposome
Brain delivery
Blood–brain barrier

ABSTRACT

Delivery of drugs to the brain is a major challenge due to the presence of the blood–brain barrier (BBB). The cell penetrating peptide TAT, which appears to enter cells with alacrity, can pass through the BBB efficiently. With this in mind, a novel TAT-modified liposome (TAT-LIP) was developed for overcoming the ineffective delivery of normal drug formulation to the brain. Targeting liposomal formulations are always composed of modified phospholipids as an anchor. However, cholesterol, another liposomal component, which was more stable and cheaper, has not been fully investigated as an alternative anchor. In this study, TAT was covalently conjugated with the cholesterol to prepare the liposome. The cellular uptake by brain capillary endothelial cells (BCECs) of rats and the mechanism of TAT-LIP pathway of endocytosis was explored. The blood brain barrier model *in vitro* was established to evaluate the transendothelial ability crossing the BBB and its transport mechanism. The biodistribution of each formulation was further identified. The results showed that the positive charge of the TAT-LIP played an important role in enhancing its brain delivery. The absorptive endocytosis might be one of the mechanisms of TAT-LIP crossing the BBB. In conclusion, the experimental data *in vitro* and *in vivo* indicated that the TAT-LIP was a promising brain drug delivery system due to its high delivery efficiency across the BBB.

1. Introduction

Central nervous system (CNS) diseases such as brain tumor, epilepsy, and neurodegenerative disorders have become one of the most dangerous threatens to the health of the human. Delivery of drugs to the brain is a major challenge due to the presence of the blood–brain barrier (BBB). The BBB is a unique, selective barrier formed by the endothelial cells that line cerebral capillaries, together with perivascular elements such as closely associated astrocytic end-feet processes, perivascular neurons and pericytes (Cecchell et al., 2007; Newton, 2006). It is a dynamic and complex interface between blood and the central nervous system that strictly controls the exchanges between the blood and brain compartments, therefore playing a key role in brain homeostasis and providing protection against many toxic compounds and pathogens (Cardoso et al., 2010). Nearly 98% of small molecules and 100% of large molecules are prevented to be uptaken by the BBB (William and Pardridge, 2005). Many potential drugs, which are effective at their site of action, have failed and have been discarded during their development for clinical use due to the failure to deliver them in sufficient quantity to the CNS. In consequence, many diseases of the CNS are undertreated.

Various strategies have been developed that can achieve BBB penetration (Temsamani and Scherrmann, 2003; Pardridge, 1994), including neurosurgery-based strategies (Temsamani and Vidal, 2004), pharmacology-based strategies, and physiology-based strategies. However, problems have been encountered with in many of these approaches (Temsamani and Vidal, 2004; Pardridge, 2002). Therefore, new and non-invasive methods are urgently needed. An alternative approach, which overcomes many of the drawbacks of the existing methods, is the use of CPPs. Several cell-penetrating peptides, which appear to enter cells with alacrity, have been developed recently (Wadia and Dowdy, 2002; Zhao and Weissleder, 2004). At present, little is known about the mechanism by which these peptides can cross the cell membrane. Some studies suggest that the peptides by virtue of their structure are able

* Corresponding author.
** Corresponding author. Tel.: +86 28 85502532; fax: +86 28 85502532.
E-mail addresses: liuji6103@163.com (J. Liu), qinhe@scu.edu.cn, qinhe317@126.com (Q. He).

0378-5173/$ – see front matter © 2011 Elsevier B.V. All rights reserved.
doi:10.1016/j.ijpharm.2011.07.021

to "worm" their way directly through the cell membrane (Derossi et al., 1996; Vivès et al., 1997). They may thus be able to penetrate the cell membrane without causing damage.

One of these cell-penetrating peptides, transactivating-transduction (TAT), is the trans-activating protein of the human immunodeficiency virus type-1 and is essential for viral replication (Banks et al., 2005). TAT contains a basic region consisting of six arginine and two lysine residues (Loret et al., 1991). Their cationic charges facilitate interaction with the normally negatively charged BBB, triggering permeabilization of the cell membrane via a receptor/transporter independent pathway which results in endocytosis of the sequence (Derossi et al., 1996). TAT showed to cross the BBB and accumulated in the CNS (Banks et al., 2005). No saturable component to transport was found for either the influx or efflux of TAT. TAT has been shown to carry heterologous proteins into several cell types (Fawell et al., 1994) and carry protein, nanoparticles, quantum dots across the BBB (Schwarze et al., 1999; Liu et al., 2008; Santra et al., 2005).

Liposomes coating with polyethylene glycol (PEG) has been proved to be very successful as a drug carrier system. It is known that PEG-modified liposomes have long-circulating characteristics through avoidance of getting trapped by the reticuloendothelial system (RES) such as liver and spleen (Lasic, 1996). Phospholipids have been extensively evaluated as an anchor for both PEGylation and receptor-targeting in liposomal formulations. Cholesterol is another important component in biomembranes. However, it has always being neglected as an alternative anchor. Cholesterol as an anchor may have advantages over DSPE (Zhao et al., 2007). Firstly, incorporation of DSPE as a lipid anchor introduces a negative charge to the liposome surface, which may lead to additional plasma protein binding (Miller et al., 1998). In contrast, cholesterol, a neutral molecule and component of most liposome formulations, is electrically neutral. Secondly, DSPE molecule is not as chemically stable as cholesterol and is susceptible to degradation during the storage (Parr et al., 1994). Thirdly, the cost of DSPE is more than 100 times higher than that of cholesterol, which is less desirable for product development. Thus, the replacement of DSPE with cholesterol is potentially more cost effective (Zhao et al., 2007).

In this study, TAT modified cholesterol was used to prepare the liposome to enhance the brain delivery. The brain targeting efficiency of TAT-LIP was evaluated *in vitro* and *in vivo*. Furthermore, the mechanism of TAT-LIP pathway was explored.

2. Materials and methods

2.1. Materials and animals

Soybean phospholipids (SPC) and cholesterol (CHO) were purchased from Bio Life Science & Technology Co., Ltd. Shanghai, PR China. Dioleoyl phosphatidylethanol-amines (DOPE) and rhodamine-phosphatidylethanolamine (Rho-PE) were purchased from Avanti Lipids (USA). NH_2-PEG_{2000}-Mal and $mPEG_{2000}$-NH_2 were all purchased from JenKem Technology (Beijing, China). TAT peptide with terminal cysteine (Cys-AYGRKKRRQRRR) was synthesized according to the standard solid phase peptide synthesis by Chengdu KaiJie Bio-pharmaceutical Co., Ltd. (Chengdu, China). Coumarin-6 and didecyldimethylammonium bromide (DDAB) were all purchased from the Sigma–Aldrich (USA). DIR was purchased from Biotium (USA). The BCA protein assay kit was purchased from Pierce (USA). The other chemicals were obtained from commercial sources.

The brain capillary endothelial cells (BCECs) and astrocyte cells (ACs) of rats were cultured primarily.

Kunming mice and Wistar rats were purchased from Experiment Animal Center of Sichuan University (PR China). All animal procedures for this study were approved by the Experiment Animal Administrative Committee of Sichuan University.

2.2. Synthesis of CHO–PEG_{2000}–TAT and CHO–$mPEG_{2000}$

Cholesteryl chloroformate was reacted with NH_2-PEG_{2000}-Mal (molar ratio = 2:1) in dry dichloromethane (DCM) at room temperature under argon in the presence of triethylamine (TEA) and 4-dimethylaminopyridine (DMAP) for about 4 h. After thin layer chromatography (TLC) showed the disappearance of NH_2-PEG_{2000}-Mal, the reaction mixture was filtered and the filtrate was evaporated under vacuum. The residue was purified on a silica-gel chromatography column (DCM:MeOH = 1:1) to get CHO–PEG_{2000}-Mal. CHO–PEG_{2000}-Mal and Cys-TAT (molar ratio = 1:1.5) were reacted in the mixture of $CHCl_3$/MeOH (v:v = 2:1) with gentle stirring at room temperature over night. After TLC showed the disappearance of CHO–PEG_{2000}-Mal, the mixture was evaporated under vacuum, the residue was redissolved by $CHCl_3$, and the insoluble material was filtered, the supernatant (CHO–PEG_{2000}–TAT) was evaporated again under vacuum and stored under −20 °C until use (Fig. 1).

The CHO–$mPEG_{2000}$ was synthesized as described above with a little modification. NH_2-$mPEG_{2000}$ was used to react with the Cholesteryl chloroformate instead of NH_2-PEG_{2000}-Mal.

2.3. Preparation of the liposomes

Rho-labeled liposomes were prepared by the thin film-hydration method. Various amounts of lipid materials were dissolved in chloroform (Table 1). Chloroform was then removed by rotary evaporation. The obtained lipidic thin film was kept in vacuum for over 6 h to completely remove the residual organic solvent. The thin film was hydrated in 5% glucose solution (pH 7.2) for 1 h at 37 °C. Then it was further intermittently sonicated by a probe sonicator at 100 W for 50 s.

Rho-labeled liposomes with different amounts of CHO–PEG_{2000}–TAT and different amounts of CHO–$mPEG_{2000}$ were prepared as Table 1 to select the optima prescription of TAT-LIP. Conventional liposome (LIP), long circulating liposome (LLIP) and cationic liposome (CL) were evaluated as the controls in this study (Table 1).

Coumarin-6-loaded liposomes and DIR-labeled liposomes were prepared as the method described above. Various amounts of lipid materials and coumarin-6/DIR were dissolved in chloroform. Following operations were the same as the Rho-labeled liposomes. The final concentration of coumarin-6 and DIR of the liposome was 10 μg/ml and 20 μg/ml respectively.

The mean size and zeta-potential of the LIP, LLIP, CL, and TAT-LIP were detected by Malvern Zetasizer Nano ZS90 (Malvern Instruments Ltd., UK).

2.4. Stability of liposomes in the presence of fetal bovine serum (FBS)

In order to choose the optimal amount of CHO–$mPEG_{2000}$, 100 μl of liposomes with different amounts of CHO–$mPEG_{2000}$ (prepared as Table 1) were added to 1 ml culture medium containing 10% FBS, and incubated at 37 °C (Chertok et al., 2009). At different time points, the size change was determined by Malvern Zetasizer Nano ZS90 (Malvern Instruments Ltd., UK).

In order to investigate the stability of the TAT-LIP and other control groups, 100 μl of LIP, LLIP, CL, and TAT-LIP were added to 1 ml culture medium containing 10% FBS to evaluate the variations in size.

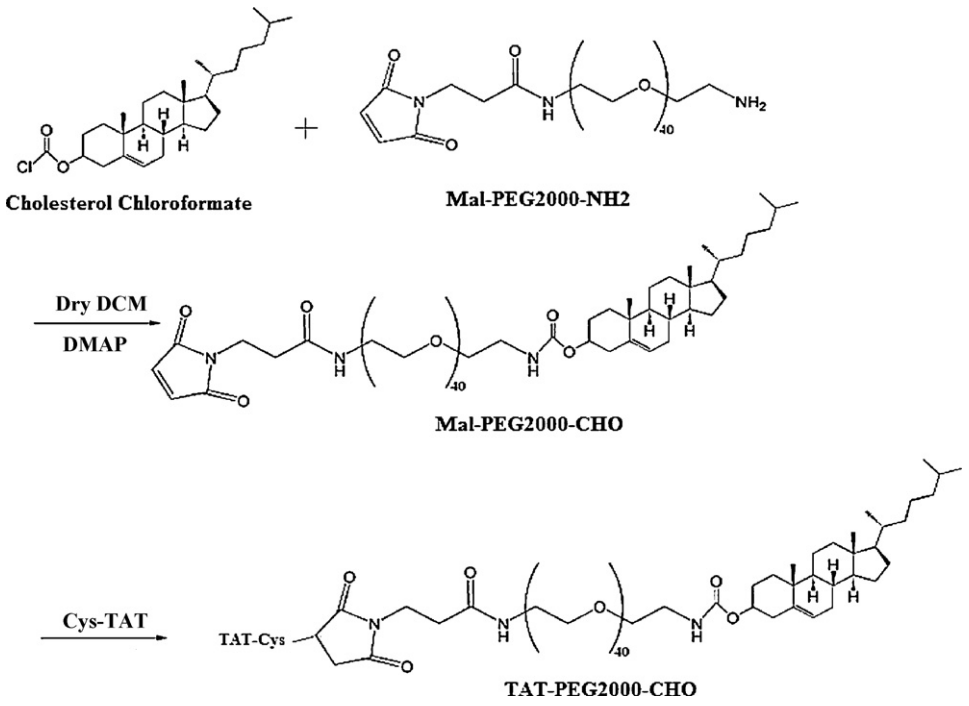

Fig. 1. Schematic of synthesis of CHO–PEG_{2000}–TAT.

2.5. Cellular uptake

2.5.1. Quantitative evaluation of cellular uptake

BCECs were plated on gelatin-coated 24-well culture plates and cultured for 48 h. Rho-labeled liposomes with different amounts of CHO–PEG_{2000}–TAT or CHO–$mPEG_{2000}$ were added to the plates at the amount of 0.12 μmol/ml. After incubation at 37 °C under 5% CO_2 for 1 h, the cells were washed three times with cold PBS and incubated with 1 ml/well 1% Triton-X 100 for 30 min at 37 °C. 100 μl of the lysate was used for the total protein of cells by BCA assay kit, the rest was added with 2.9 ml 1% Triton-X 100 and used to determine the cell-associated fluorescence at Ex = 560 nm, Em = 578 nm respectively on a spectrofluorimeter (RF-5301 fluorospectrophotometry, Shimadzu, Japan), the results were expressed as the Uptake Indices (UI) which was expressed as fluorescence/μg of protein.

In order to compare the cellular uptake of TAT-LIP with other controls (LIP, LLIP, CL), the BCECs were incubated with Rho-labeled liposomes which were diluted with FBS-free medium or medium containing 10% FBS to different final concentrations of total lipid (0.06 μmol/ml, 0.12 μmol/ml, 0.24 μmol/ml) for 60 min at 37 °C. In a separate experiment, to study the effects of incubation time on liposomes cellular uptake, the cells were incubated with Rho-labeled liposomes of a final concentration of 0.12 μmol/ml for 1 h, 4 h and 8 h at 37 °C. At the end of the incubation period, the cells were washed with ice-cold PBS for three times, and treated as described above.

2.5.2. Confocal laser scanning microscopy (CLSM)

The Rho-labeled liposomes were prepared as described above. BCECs were plated on gelatin-coated cover slips in 6-well culture plates and cultured for 48 h. Different formulations (LIP, LLIP, CL,

Table 1
Various formulations of liposomes.

Type of liposomes	Composition of liposomes (molar ratio)						
	SPC	CHO	CHO–PEG_{2000}	CHO–PEG_{2000}–TAT	DDAB	DOPE	Rho-PE
Liposomes with different amounts of CHO–$mPEG_{2000}$–TAT							
3% PEG + 0% TAT	2 equiv.	0.91 equiv.	0.09 equiv.	–	–	–	4 μg/ml
3% PEG + 1% TAT	2 equiv.	0.88 equiv.	0.09 equiv.	0.03 equiv.	–	–	4 μg/ml
3% PEG + 3% TAT	2 equiv.	0.82 equiv.	0.09 equiv.	0.09 equiv.	–	–	4 μg/ml
3% PEG + 5% TAT	2 equiv.	0.76 equiv.	0.09 equiv.	0.15 equiv.	–	–	4 μg/ml
3% PEG + 8% TAT	2 equiv.	0.67 equiv.	0.09 equiv.	0.24 equiv.	–	–	4 μg/ml
3% PEG + 10% TAT	2 equiv.	0.61 equiv.	0.09 equiv.	0.3 equiv.	–	–	4 μg/ml
Liposomes with different amounts of CHO–$mPEG_{2000}$							
0% PEG + 5% TAT	2 equiv.	0.85 equiv.	–	0.15 equiv.	–	–	4 μg/ml
1% PEG + 5% TAT	2 equiv.	0.82 equiv.	0.03 equiv.	0.15 equiv.	–	–	4 μg/ml
3% PEG + 5% TAT	2 equiv.	0.76 equiv.	0.09 equiv.	0.15 equiv.	–	–	4 μg/ml
5% PEG + 5% TAT	2 equiv.	0.7 equiv.	0.15 equiv.	0.15 equiv.	–	–	4 μg/ml
8% PEG + 5% TAT	2 equiv.	0.61 equiv.	0.24 equiv.	0.15 equiv.	–	–	4 μg/ml
10% PEG + 5% TAT	2 equiv.	0.55 equiv.	0.3 equiv.	0.15 equiv.	–	–	4 μg/ml
Study groups							
LIP	2 equiv.	1 equiv.	–	–	–	–	4 μg/ml
LLIP (8% PEG)	2 equiv.	0.76 equiv.	0.24 equiv.	–	–	–	4 μg/ml
CL	–	–	–	–	2 equiv.	1 equiv.	4 μg/ml
TAT-LIP (3% PEG + 5% TAT)	2 equiv.	0.76 equiv.	0.09 equiv.	0.15 equiv.	–	–	4 μg/ml

and TAT-LIP) were added to the plates with a total lipid concentration of 0.12 μmol/ml. After incubation at 37 °C under 5% CO_2 for 1 h, 2 ml 2 μg/ml DAPI was added for 5 min, cells were washed three times with cold PBS and fixed using 4% paraformaldehyde. Cover slips were mounted cell-side down with slides and viewed using a Leica TCS SP5 AOBS confocal microscopy system (Leica, Germany).

2.5.3. Cellular uptake mechanism of TAT-LIP on BCECs

The effect of temperature on TAT-LIP uptake was performed at 4 °C and 37 °C. To study the effect of various inhibitors on their cellular uptake, the cells were pre-incubated with the following inhibitors (Kheirolomoom and Ferrara, 2007; Chen et al., 2010) at 37 °C for 30 min: sodium azide (0.1%, w/v), filipin (10 μg/ml), oxophenylarsine (PHAsO) (10 μM), colchicine (10 Mm), sucrose (400 mM), heparin (100 U/ml and 20 U/ml), TAT (5 mg/ml and 1 mg/ml), and polylysine (500 μg/ml and 100 μg/ml). Following the pre-incubation, Rho-labeled TAT-LIP with a total lipid concentration of 0.12 μmol/ml was added and the incubation was continued at 37 °C for 1 h. At the end of the incubation period, the cells were washed with ice-cold PBS for three times. Subsequently, the cells were treated as described in Section 2.5.1.

2.6. Cytotoxicity

Microtiter tetrazolium (MTT) assay was performed according to a standard MTT-based colorimetric assay. Briefly, BCECs were seeded onto 96-well plates. 48 h later, fresh medium containing serial concentrations of various drug formulations, including LIP, LLIP, CL, and TAT-LIP, were given different concentrations of lipids ranging from 75 nmol/ml to 1.2 μmol/ml of lipids. Cells incubated in medium without any drugs were used as blank controls. After incubating for 12 h, the liposomes were moves away, 20 μl per well 3-(4,5-dimethylthiazol-2-yl)-2,5-diphenyl tetrazolium bromide (5 mg/ml) was added. The plates were incubated for an additional 4 h. The cells were lysed using 200 μl of dimethylsulfoxide (DMSO) solution, and placed in the incubator at 37 °C for 15 min. The absorbance values of the lysed cells were read on a microplate reader (BIO-RAD model 550, Bio-Rad, USA) at the wavelength of 570 nm. The survival percentages were calculated using the following formula: survival ratio (%) [(A570 for the treated cells)/(A570 for the control cells)] × 100, where A570 is the absorbance value.

2.7. Transendothelial ability and mechanism of Rho-labeled liposomes on in vitro BBB model

The study of transendothelial ability and mechanism was performed according to previous reports (Lu et al., 2005). Ringer-HEPES (150 mM NaCl, 5.2 mM KCl, 2.2 mM $CaCl_2$, 0.2 mM $MgCl_2$, 6 mM $NaHCO_3$, 2.8 mM glucose, 5 mM HEPES; pH 7.4) was added to the acceptor chamber of 24-well plate (1 ml per well). After pre-incubating with Ringer-HEPES for 15 min, 200 μl of Rho-labeled liposomes in Ringer-HEPES solution with a total lipid concentration of 240 nmol were added to the donor chamber, respectively. The incubations were performed at 37 °C. At 15 min, 30 min, 60 min, 90 min, 2 h, 3 h, 4 h, 5 h and 6 h, the Rho-labeled liposome in acceptor chamber was assayed by RF-5301 fluorospectrophotometry (Ex = 560 nm, Em = 578 nm, Shimadzu, Japan). Triplicate samples were performed. The accumulated permeating volume was indicated by dividing the accumulated amount of lipids recovered in the abluminal side by its initial concentration in the luminal side (Siflinger-Birnboim et al., 1987).

To study the effect of various inhibitors on the transendothelial profile of the TAT-LIP, *in vitro* BBB model was used. Following inhibitors were added in the donor chamber and incubated with cells at 37 °C for 30 min: (1) TAT (5 mg/ml or 1 mg/ml); (2) heparin (100 U/ml or 20 U/ml); (3) polylysine (500 μg/ml or 100 μg/ml). Following the pre-incubation, the study of transport was performed the same as above.

2.8. Bio-distribution in vivo

2.8.1. Ex vivo NIR fluorescence imaging

For *ex vivo* optical imaging, mice were injected intravenously with DIR-loaded liposomes (Pharm et al., 2005). *Ex vivo* NIR fluorescence imaging was performed 1 h after probe injection. Animals were perfused with 0.9% sodium chloride solution from the heart and sacrificed. The whole brains were removed and frozen as quickly as possible. The frozen brains were then cut into frozen coronal sections of approximately 1 mm thickness, and placed into imaging system (Imaging Station IS2000MM, Kodak), equipped with a band-pass filter at 770 nm and a long pass filter at 830 nm. Images were captured by the CCD camera embedded in the imaging.

2.8.2. Quantitative study of bio-distribution

All procedures of the *in vivo* studies were approved by Sichuan University animal ethical experimentation committee, according to the requirements of the National Act on the use of experimental animals (People's Republic of China).

96 mice were randomly assigned to four groups; each was then divided into 8 time point groups. LIP, LLIP, CL, and TAT-LIP were given to the mice via the tail veins; each was equivalent to the administration dose of coumarin-6 of 0.1 mg/kg. At 15 min, 30 min, 1 h, 2 h, 4 h, 8 h, 12 h, and 24 h after injection, the animals were sacrificed by cervical dislocation, and the organs (heart, liver, spleen, lung, kidney, and brain) were removed and flushed with water for three times to remove the blood remained (Han et al., 2006). All the tissues were homogenized with triple amount of water. 10 μl of internal standard (coumarin-7) was added into 200 μl organ homogenate, and extracted with 1 ml N-hexane. The mixture was vortexed for 5 min, and centrifuged at 10,000 rpm for 5 min. The supernatant was transferred to another centrifuge tube, and dried under air stream at room temperature. The dry residue was reconstituted with 50 μl of methanol. The solution was centrifuged at 12,000 rpm for 10 min, and then 20 μl of the supernatant was injected into the HPLC system for analysis. A reversed-phase HPLC was employed for the determination of coumarin-6 concentrations in the tissue samples. A HPLC (Alltech, Illinois, USA) system with a Diamonsil C_{18} column (200 mm × 4.6 mm, 5 μm), and a mixture of methanol–water (92:8) as mobile phase was employed for the *in vivo* studies. The concentrations of coumarin-6 were analyzed by fluorescence detector with Ex 465 nm and Em 502 nm. The column temperature was 35 °C.

The area under the concentration–time profile (AUC_{0-t}), maximal concentration (C_{max}) of brain was calculated by Data and max Statistics (DAS, Shanghai, China). The relative uptake efficiency (RE) and concentration efficiency (CE) were calculated to evaluate the brain targeting property of liposome. The values of RE and CE were defined as follow (Chen et al., 2009):

$$RE = \frac{(AUC_{0-t})s}{(AUC_{0-t})c}$$

$$CE = \frac{(C_{max})s}{(C_{max})c}$$

where *s* and *c* represent sample (TAT-LIP) and controls (LIP, LLIP, and CL), respectively.

2.8.3. Distribution of coumarin-6 loaded liposomes in specific brain regions of rats

Adult, male Wistar rats (180 ± 20 g body weight) were injected with coumarin-6-loaded LIP, LLIP, CL, and TAT-LIP into the caudal veins (dose 0.1 mg/kg of coumarin-6, $n = 3$). 1 h later, the animals

were perfused with N.S. from the heart and sacrificed. The brains were removed and quickly washed with cold deionized water, then isolated into the following regions (Banks et al., 2005): the cerebral cortex, hippocampus, striatum, cerebellum, and brainstem. Subsequently, the regional brain tissues were subjected to n-hexane extraction and analyzed by HPLC-fluorescence (Alltech Technology Co., Ltd., Chengdu, China) with coumarin-7 as internal standard (Qin et al., 2010).

3. Results

3.1. Synthesis of CHO–PEG$_{2000}$–TAT/CHO–mPEG$_{2000}$

To construct the liposomal drug delivery system, we conjugated TAT to the distal end of PEG$_{2000}$ anchored to cholesterol. In the ^{1}H NMR spectrum of CHO–PEG$_{2000}$-Mal, ^{1}H NMR ($CDCl_3$, 400 MHz) δ (ppm): 6.70 (s, 2H), 5.31 (d, 1H), 3.80–3.30 (br, m, PEG protons, ~181H), 2.30 (d, 2H), 1.50–0.82 (m, Chol protons), with 0.63 (s, 3H), 0.86 (d, 6H), 0.92 (d, 3H,), 0.99 (s, 3H). MS (m/z) confirmed the formation of CHO–PEG$_{2000}$–TAT (Mw observed = 4208, Mw calculated = 4255). CHO–mPEG$_{2000}$ was synthesized as described above, TLC showed the purity of CHO–mPEG$_{2000}$ >95%.

3.2. The optimizing prescription of TAT-LIP

The cellular uptake of liposomes with different amounts of CHO–PEG$_{2000}$–TAT showed obvious distinction among each other. The sizes of liposomes with different amounts of CHO–PEG$_{2000}$–TAT were all below 200 nm, PDI were smaller than 0.3. The Uptake Indices of liposomes modified with 5% CHO–PEG$_{2000}$–TAT was much higher than liposomes without CHO–PEG$_{2000}$–TAT or with 1% and 3% CHO–PEG$_{2000}$–TAT. The cellular Uptake Indices of liposomes with 8% and 10% CHO–PEG$_{2000}$–TAT was almost the same with the liposomes modified with 5% (Fig. 2). So the 5% was chosen as the optimal ratio of CHO–PEG$_{2000}$–TAT.

Fig. 3 shows that 0–3% of CHO–mPEG$_{2000}$ did not affect the cellular uptake of liposome. However, the Uptake Indices decreased obviously when the amount of CHO–mPEG$_{2000}$ was more than 5%.

The stability experiment showed that the size of liposomes without CHO–mPEG$_{2000}$ changed distinctly during 8 h. In the first 10 min, the size of it became more than 1000 nm. The size of liposomes with 1% CHO–mPEG$_{2000}$ varied from 173.5 nm to 397.7 nm during 8 h. Liposomes with more than 3% CHO–mPEG$_{2000}$ were stable in the serum, whose sizes were all below 200 nm. So the liposomes contained 3% CHO–mPEG$_{2000}$ would not decrease the cellular uptake, and it also maintained good stability in the serum.

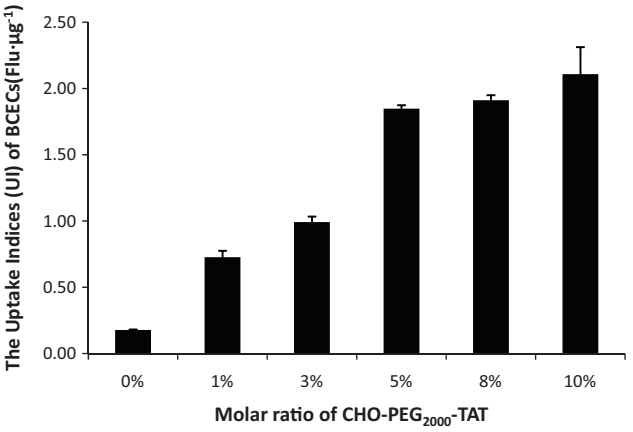

Fig. 2. Quantitative observation of effect of different amounts of CHO–PEG$_{2000}$–TAT on the uptake of Rho-labeled liposomes by BCECs.

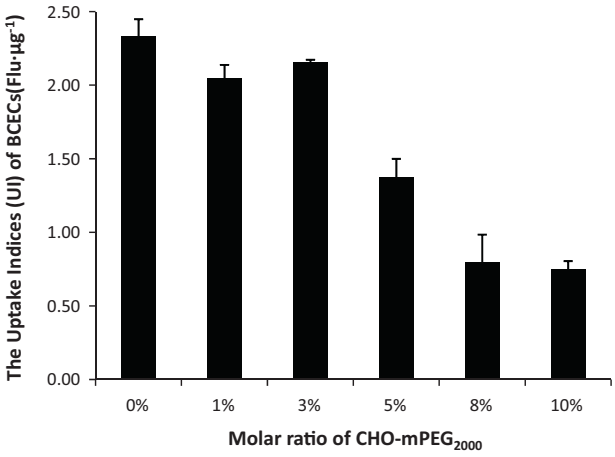

Fig. 3. Quantitative observation of effect of different amounts of CHO–mPEG$_{2000}$ on the uptake of Rho-labeled liposomes by BCECs.

3.3. Characterization and stability of the liposomes

For the four types of liposomes, the average particle sizes were less than 150 nm. The values of charge distributing around the liposomes vesicles were shown in Table 2. The LIP and the LLIP were negative charged. The TAT-LIP was slightly positive charged. The positive charge of CL was much higher than that of TAT-LIP.

The stability data showed that the LIP, LLIP, TAT-LIP were mainly below 150 nm during 8 h in the culture medium with 10% FBS, while the size of CL was over 500 nm 15 min later.

3.4. Quantitative analysis of cellular uptake

The cellular uptake of each formulation by BCECs was in a concentration-dependent manner within 8 h (Fig. 4A). The Uptake Indices of TAT-LIP were 13.03, 6.96, and 6.71 times higher than those of LIP; 12.49, 15.44, and 12.78 times higher than those of LLIP; 4.05, 1.44 and 1.52 times higher than those of CL at 0.06 μmol, 0.12 μmol, and 0.24 μmol of lipids in the medium contained 10% FBS, respectively. In the serum free medium, they were 5.29, 2.27 and 2.24 times higher than those of LIP; 7.82, 6.62, and 3.05 times higher than those of LLIP; 1.07, 0.80, and 0.86 times higher than those of CL, respectively.

The cellular uptake of each formulation by BCECs was also in a time-dependent manner within 8 h (Fig. 4B). The Uptake Indices of TAT-LIP were 6.96, 3.91, and 3.82 times higher than those of LIP; 15.44, 7.27, and 5.36 times higher than those of LLIP; 1.44, 1.45, and 1.78 times higher than those of CL at 1 h, 4 h, and 8 h in the medium contained 10% FBS, respectively. In the serum free medium, they were 2.27, 2.66, and 2.13 times higher than those of LIP; 6.62, 3.76, and 2.66 times higher than those of LLIP; 0.80, 0.47, and 0.40 times higher than those of CL, respectively.

3.5. Confocal laser scanning microscopy (CLSM)

After 1 h of incubation, both liposomal labels were localized at the plasma membrane and the cytoplasm of the BCECs. The cell

Table 2
Size and zeta potential of each liposome (n = 3).

	LIP	LLIP	CL	TAT-LIP
Size (nm)	143.4 ± 0.8	119.7 ± 0.6	89.1 ± 6.1	147.6 ± 0.6
PDI	0.262 ± 0.002	0.210 ± 0.009	0.276 ± 0.018	0.207 ± 0.018
Zeta (mV)	−22.66 ± 1.53	−8.00 ± 1.55	36.37 ± 2.31	3.87 ± 1.13

Data represented the mean ± SD (n = 3).

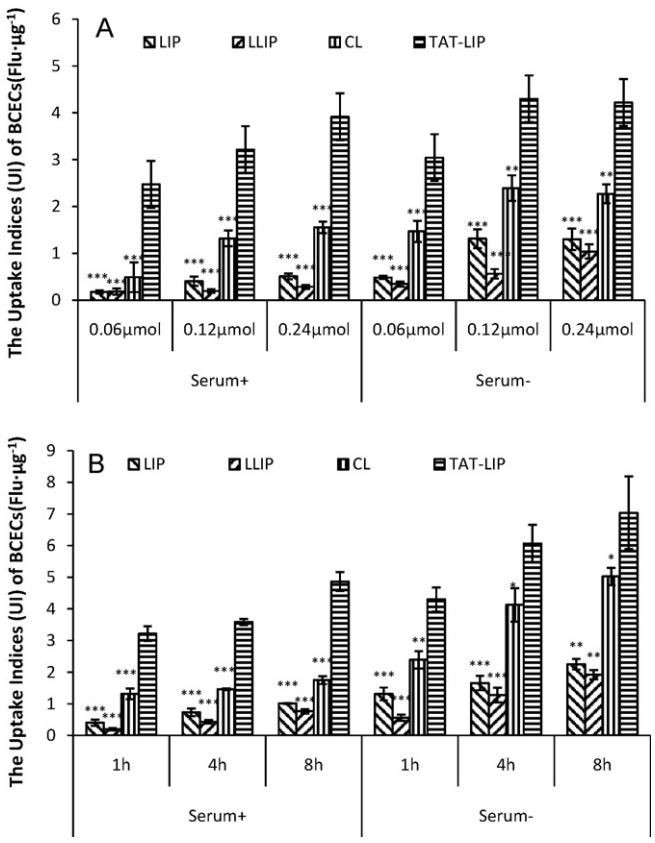

Fig. 4. Quantitative evaluation of cellular uptake. The cellular uptake was expressed as the Uptake Indices ($n = 3$). (A) The cellular uptake was measured 1 h after treated with different concentrations of each liposome within or without serum ($n = 3$). (B) The cell uptake was measured 1, 4, and 8 h after treated with the same concentration (0.12 μmol/ml) of different liposomes within or without serum. Data represented the mean ± SD ($n = 3$). $^{*}P < 0.05$; $^{**}P < 0.01$; $^{***}P < 0.001$; versus TAT-LIP.

nucleuses were stained blue with DAPI. The red fluorescence could be found around the cell nucleus. Among all four kinds of liposomes, the internalization of liposomes modified with TAT by the BCECs was the most evident (Fig. 5). The fluorescence exhibited by the BCECs was markedly decreased which were treated with LIP and LLIP. The LLIP showed the poorest cellular uptake.

3.6. Uptake mechanism of TAT-LIP on BCECs

To determine whether the TAT-modified liposomes under investigation in this study follow an energy dependent or independent pathway, the cellular uptake of TAT-LIP was evaluated at 4 °C or in the presence of metabolic inhibitors (sodium azide). Fig. 6A shows that after incubation at 37 °C, the TAT-LIP was efficiently uptaken by the cells. However, compared with the controls, the cellular uptake of TAT-LIP decreased significantly when incubated at 4 °C or in the presence of sodium azide at 37 °C. The cellular uptake of TAT-LIP at 4 °C and in the presence of sodium azide at 37 °C decreased by 33.63% and 45.8%, respectively (Fig. 6A).

Different inhibitors of endocytosis were further used to reveal the pathways involved in the uptake of TAT-LIP by BCECs. The cellular uptake of TAT-LIP was inhibited at different extents with the exposure to different inhibitors (Fig. 6B). Compared with the controls, treatment with filipin, PHAsO, colchicines, and sucrose significantly decreased the uptake of TAT-LIP by 16.36%, 33.52%, 31.32%, and 35.61%, respectively ($P < 0.05$).

Ionic inhibitors (heparin and polylysine) and excess free TAT were pre-incubated with the cells to investigate the contribution of the positive charge of TAT-LIP to the association of their uptake by BCECs. The ionic inhibitors significantly inhibited the cellular uptake of TAT-LIP in a similar profile (Fig. 6C). The uptake of TAT-LIP decreased by 84.73%, 78.01%, 79.84%, 86.04%, 23.42%, and 27.36% after treated by 20 U/ml and 100 U/ml of heparin, 100 μg/ml and 500 μg/ml of polylysine, 1 mg/ml and 5 mg/ml TAT, respectively. The uptake inhibition of TAT-LIP induced by excess free TAT was not more significant than that of other ionic inhibitors.

3.7. Cytotoxicity

Several groups have reported a significant cytotoxicity of free TAT peptides (Brooks et al., 2005). Therefore, we characterized the cytotoxicity of our liposomes by measuring the mitochondrial activity. After direct exposure, effect of each liposome on the proliferation of BCECs was depicted in Fig. 7. MTT assay has showed that LIP, LLIP, and TAT-LIP exhibited little cytotoxicity on the BCECs during 12 h at the concentrations of lipids ranging from 75 nmol/ml to 150 nmol/ml (the cell survival ratio ≥70%); and showed obvious cytotoxicity on the BCECs at the concentrations of lipids ranging from 300 nmol/ml to 1200 nmol/ml (the cell survival ratio ≥55% for LIP, ≥65% for LLIP and TAT-LIP). Linking of TAT peptides to the liposome did not increase their cytotoxicity of the liposome. The CL showed obvious inhibitory effect at the amount of 15–600 nmol/ml (<30% cell survival ratio) and the strongest inhibitory effect at the amount of 1200 nmol/ml (<4% cell survival ratio).

3.8. Transendothelial ability of Rho-labeled liposomes on BBB model in vitro

BBB model was constructed according to the previous study (Lu et al., 2005) by co-culturing BCECs and ACs. By measuring transendothelial electrical resistance (TEER) primarily (>250 Ω cm^2), they were employed to evaluate the transport of various formulations across the BBB model *in vitro*. No obvious reduction in the TEER values was observed in LIP,LLIP, and TAT-LIP groups during this study, which indicated that the transport of drug did not disrupt the BBB barrier properties. Results had showed that the rank of accumulated cleared volume (μl) across the BBB was at 6 h. TAT-LIP showed a significant drug transport across the BBB. The transendothelial transport ability was TAT-LIP > CL > LIP > LLIP illustrated in Fig. 8. In addition, the drug transport across the BBB was time-dependent manner.

3.9. Transendothelial mechanism of Rho-labeled TAT-LIP on BCECs

To reveal the contributions of free TAT and the charge of TAT-LIP particles to their transendothelial transport across the BBB, excess free TAT and ionic inhibitors (heparin and polylysine) were used in the transendothelial transport studies. The transendothelial transport of TAT-LIP was inhibited by free TAT and ionic inhibitors (Fig. 9).

3.10. Bio-distribution in vivo

3.10.1. In vivo NIR fluorescence imaging

There was defined fluorescent signal in the brain of each group (Fig. 10). *Ex vivo* imaging was performed on excised mouse brains. A strong NIR fluorescent signal from the brain of the mouse injected intravenously with the TAT-LIP was observed 1 h after injection. Brains from control mice treated with LIP, LLIP, and CL had weaker signal compared to TAT-LIP. Control animals injected with saline solution produced no background signal, to confirm that the observed fluorescence signal was truly from the brain.

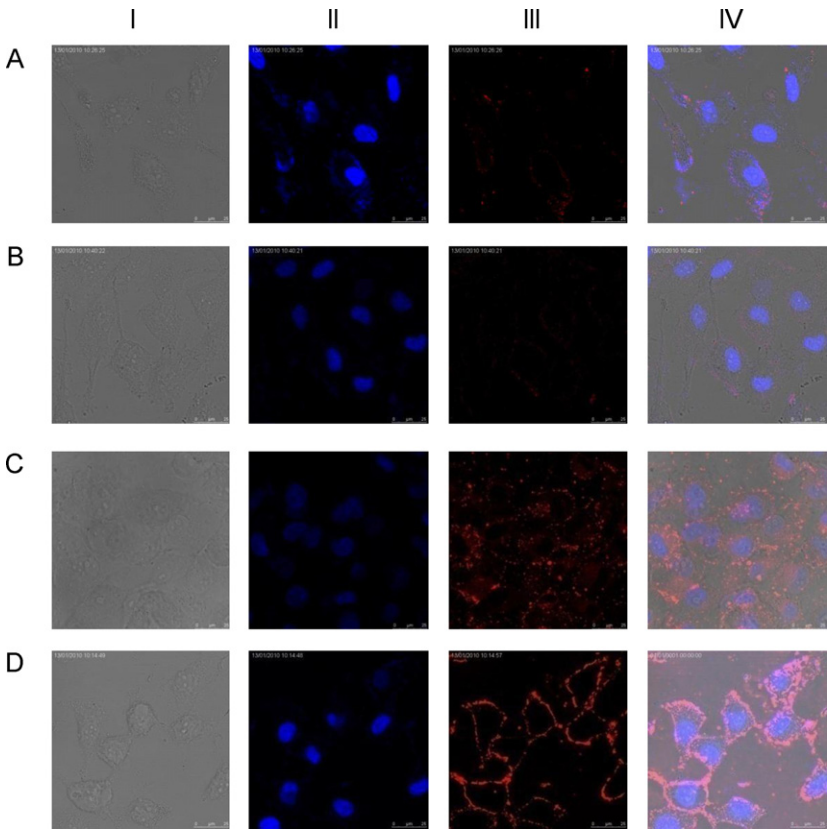

Fig. 5. Qualitative observation of the uptake of different Rho-labeled liposomes by BCECs under fluorescence microscopy. Concentration of liposomes of all samples were adjusted to 0.12 μmol of lipids each well. For each line was (A) LIP, (B) LLIP, (C) CL, and (D) TAT-LIP. The row I was the bright field, the blue fluorescence exhibited in row II was due to DAPI-staining of the nuclei. The red fluorescence exhibited in row III was due to the Rho-labeled liposomes. The forth row was the overlay sight. (For interpretation of the references to color in this figure legend, the reader is referred to the web version of the article.)

3.10.2. Quantitative study of bio-distribution

To further evaluate the possibility of the TAT-LIP being transported across BBB, the tissue distribution of LIP, LLIP, CL, and TAT-LIP were studied. The tissue distribution of coumarin-6 was measured at 15 min, 30 min, 1 h, 2 h, 4 h, 8 h, 12 h, and 24 h after i.v. injection.

Coumarin-6 distributed in tissues could be completely separated and detected under the selected analytical method, which could be validated by the standard curves (r of all tissues > 0.995), and the recoveries were between 85% and 115% in all tested tissues.

After i.v. administration of LIP, LLIP, CL, and TAT-LIP, the pharmacokinetic parameters, RE and CE of coumarin-6 in brain were reported in Table 3. In brain, the AUC_{0-t} of coumarin-6 for TAT-LIP was 2.54 times that of LIP, 1.88 times that of LLIP, and 1.79 times that of CL. The C_{max} of TAT-LIP was 2.01 times that of LIP, 1.57 times that of LLIP, and 1.91 times that of CL. The biodistribution of coumarin-6 in each tissue at each time point was shown in Fig. 11.

Table 3
Pharmacokinetic parameters of coumarin-6 in brain following i.v. injection of LIP, LLIP, CL and TAT-LIP in mice.

PK parameters	LIP	LLIP	CL	TAT-LIP
C_{max} (h)	30.39**	40.36*	33.19*	63.37
AUC_{0-t} (μg/l h)	132.92**	179.56**	189.08*	338.00
RE	2.54	1.88	1.79	–
CE	2.01	1.57	1.91	–

Data represented the mean ± SD (n = 3).
* $P < 0.05$, versus TAT-LIP.
** $P < 0.01$, versus TAT-LIP.
*** $P < 0.001$, versus TAT-LIP.

3.10.3. Distribution of coumarin-6 loaded liposomes in specific brain regions of rats

To evaluate the possibility of the TAT-LIP being transported to the specific brain regions, the distribution of LIP, LLIP, CL, and TAT-LIP in the cerebral cortex, hippocampus, striatum, cerebellum, and brainstem was studied. After i.v. administration of LIP, LLIP, CL, and TAT-LIP, the concentration of coumarin-6 in specific brain regions was shown in Fig. 12.

The concentration of coumarin-6 in the cerebral cortex, hippocampus (HP), striatum, cerebellum, and brainstem of TAT-LIP groups were 1.47, 1.68, 0.57, 1.41,and 1.99 times higher than that of LIP; 1.37, 1.07, 0.46, 0.78, and 1.41 times higher than that of LLIP; and 1.23, 1.18, 0.77, 1.08, and 1.51 times higher than that of CL. The distribution tendency was almost the same between these four groups.

4. Discussion

The peptide TAT was modified on cholesterol, one of the components of liposomes, therefore a better stability for the ligand and a lower cost for the material were achieved compared with the modifications on phospholipid. Before this study, a comparative uptake study was conducted between liposomes prepared with TAT-modified cholesterol and TAT-modified DOPE using BCECs as the model cell. The result exhibited no difference in uptaking them by BCECs (see supplementary material). TAT was then modified on the cholesterol considering the fact that cholesterol is chemically stable and much cheaper than phospholipid. The comparative study between TAT-modified cholesterol and TAT-modified phospholipid was now under further investigation.

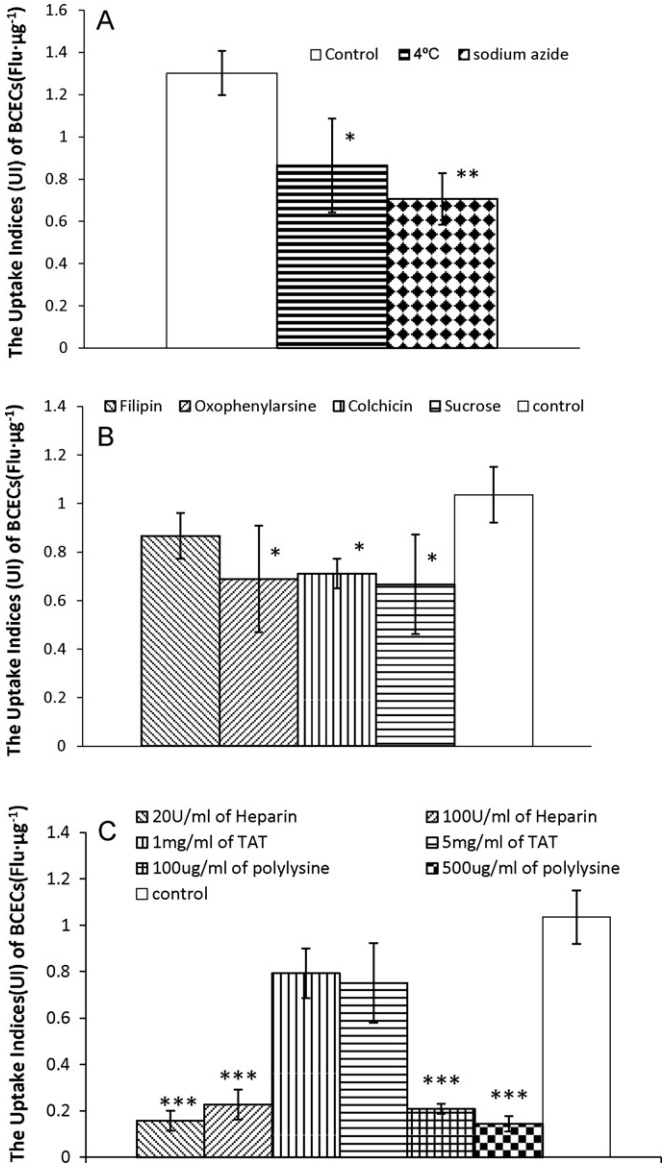

Fig. 6. Quantitative observation of cellular uptake of TAT-LIP. (A) Uptake at 4 °C and in the presence of sodium azide. (B) Uptake in the presence of different endocytosis inhibitors. (C) Uptake in the presence of different electric charge inhibitors. Data was shown as the Uptake Indices (UI). Data represented the mean ± SD ($n = 3$). *$P < 0.05$; **$P < 0.01$; ***$P < 0.001$; versus control.

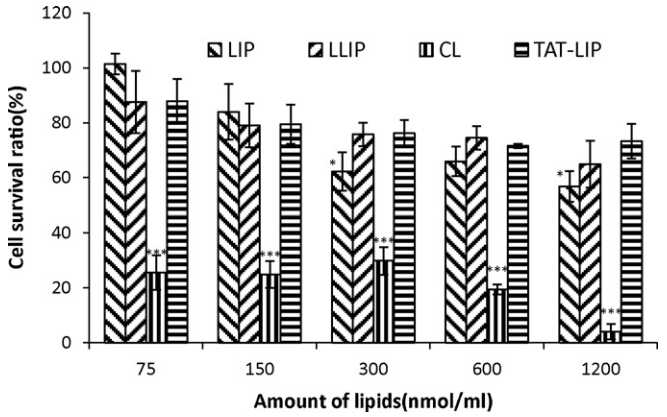

Fig. 7. Cytotoxicity on BCECs by directly applying each formulation for 12 h. Data are presented as the mean ± SD. *$P < 0.05$; **$P < 0.01$; ***$P < 0.001$; versus TAT-LIP.

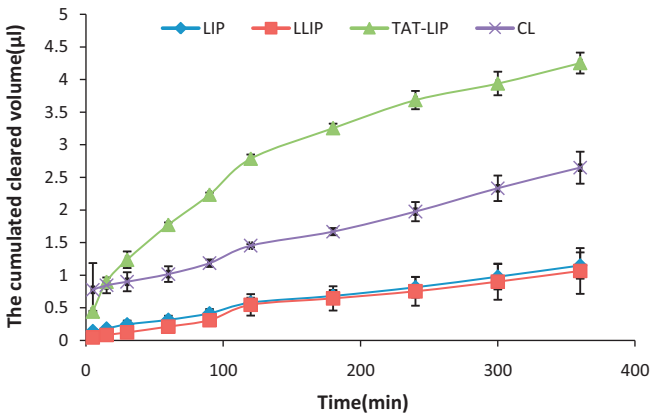

Fig. 8. Transendothelial ability of each formulation on BBB model *in vitro*. Data was shown as the accumulated cleared volume (μl) at assigned time points. Data represented the mean ± SD ($n = 3$).

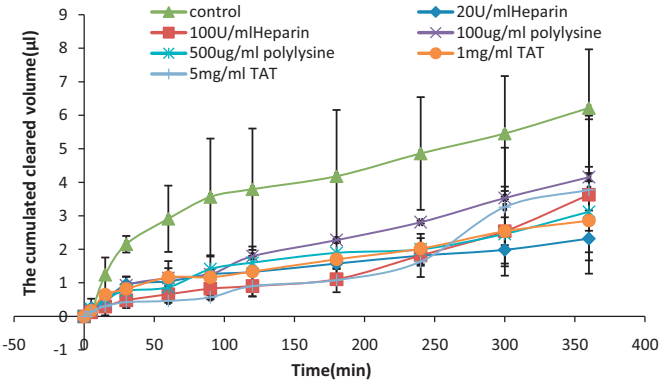

Fig. 9. Transendothelial ability of TAT-LIP on BBB model *in vitro* with different kinds of electric charge inhibitors and free TAT. Data was shown as the accumulated cleared volume (μl) at assigned time points. Data represented the mean ± SD ($n = 3$).

A pilot study on the cell uptake was conducted as to the liposomes prepared with different amounts of CHO–PEG_{2000}–TAT before a formal experimental screening for the optimum amount of TAT, and the cells were subjected to observation under fluorescent microscope over different periods of incubation time. The results validated that after 1 h of incubation, difference among each group was already obvious enough, and the uptake tendency remained the same after 2 h and 4 h of incubation. So 1 h of incubation was adopted in the quantification assays. Coupling the TAT-peptide to the outer surface of liposomes strongly increased the binding of liposomes to BCECs. The more TAT-peptide modified on the liposome, the stronger fluorescence exhibited by the cells. It could be concluded that the TAT can enhance the cellular uptake of liposomes. When the TAT was over 5% of total lipids, more TAT did little contribution to the cellular uptake. The size data and the transmission electron micrographs (see supplementary material) showed that the liposomes with different amounts of CHO–PEG_{2000}–TAT all kept the liposome structure.

Poly(ethylene glycol) (PEG) was always used to modify the surface of liposomes for improving pharmacokinetics (PK) after intravenous (i.v.) administration and minimizing their protein binding to escape the surveillance of RES (Li and Huang, 2010). In this study, PEG was used as linker to connect the cholesterol and TAT. However, the TAT modified on the surface of the liposomes might bind with the protein in the serum and decrease the stability of the liposomes. So, the CHO–$mPEG_{2000}$ was added to shield the TAT and enhance the stability of the liposomes. But the

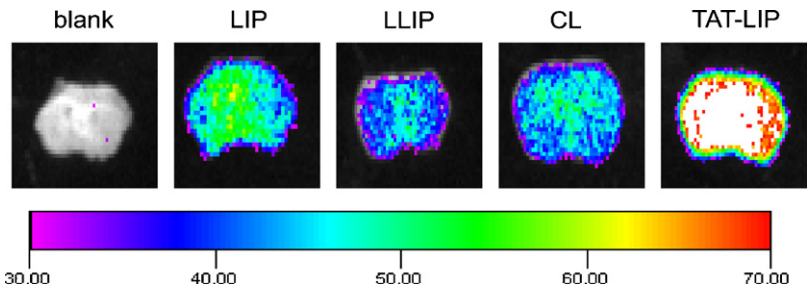

Fig. 10. *Ex vivo* imaging of brain given different liposomes via tail vein.

CHO–mPEG$_{2000}$ also restricted the cellular uptake of liposomes by BCECs. When the molarity ratio of CHO–mPEG$_{2000}$ of total lipids was over 3%, the cell Uptake Indices decreased obviously. 3% of CHO–mPEG$_{2000}$ could help maintaining good stability of the liposome while its size did not vary markedly in the culture medium with 10% FBS.

The general approach to fabricate the active-targeting liposome is interior extrapolation method, that is, to insert ligand-modified phospholipid or cholesterol into the preformed liposome, thus ensuring that the ligand and PEG distributed on the surface of liposome. In this study, the liposome was prepared by organic phase reaction method. TAT-modified cholesterol was dissolved in the chloroform with other lipids, and then the solvent was removed under reduced-pressure evaporation to obtain a thin lipid film. The film was subsequently hydrated to attain the liposome. To certify that PEG and TAT distributed on the surface of the liposome, the different capacities of BCECs to uptake liposomes prepared by organic-phase method and insertion method were explored. BCECs showed no preferences in uptaking these two preparations (see supplementary material), confirming the fact that TAT and PEG distributed on the surface of the liposome. The possible explanation for this is that the hydrophilic interior space of the liposome is quite limited, so most of the long-chain PEG remains on the surface.

There were three control groups in this study. LIP was a common control group without any modification. The LLIP had 8% of CHO–mPEG$_{2000}$. The density of PEG on its surface was the same with the TAT-LIP which contained 3% CHO–mPEG$_{2000}$ and 5% CHO–PEG$_{2000}$–TAT. As the carrier of the gene, the CL had strong transfection ability which might be due to its strong positive charge. The TAT was also weakly positively changed, but it could still pass through the cells efficiently. So the CL group was set up to identify the effect of the positive charge.

The size and the deformability of particles play a critical role in their clearance by the sinusoidal spleens of humans and rats. Particles must be either small or deformable enough to avoid the splenic filtration process at the interendothelial cell slits (IES) in the walls of venous sinuses (Kaur et al., 2008). However, the slit size rarely exceeds 200–500 nm in width, even with an erythrocyte in transit. Therefore, the size of an engineered long circulatory particle should not exceed 200 nm ideally. If larger, the particle must be deformable enough to bypass IES filtration. Alternatively, long-circulating rigid particles of greater than 200 nm may act as spleen otropic agents and removed later on, if they are not rigid. Hence liposomes of size below 200 nm have an increased blood circulation and thus an increase in the time for which the drug remains in contact with BBB and for the drug to be taken up by the brain (Chen et al., 2004). Since the particle size is an important property of particles that affects its endocytosis by the brain capillary endothelial cell, the size distribution is generally controlled under 200 nm in diameter (Hu et al., 2009).

To examine the cellular uptake of liposomes, the liposomal bilayer was fluorescently labeled with rhodamine. The cell nucleus was stained with DAPI to investigate the localization of the liposomes in the cells. The red florescence were mostly found around the cell membrane which indicated that some of liposomes were fused with the plasma membrane. Rhodamine was marked on the phospholipid of the liposomes. Liposomes underwent a partial fusion with the membranes of the cells when transporting into the cells, resulting in remarkable red fluorescent signaling on the cell membranes. In the following studies, doxorubicin with red fluorescence was able to achieve an effective delivery into the cells by liposomes.

The characteristics and behavior of different Rho-labeled liposomes were also investigated on BCECs quantitatively. The cellular uptake of TAT-LIP was improved by TAT modification compared with unmodified LLIP and LIP. The uptake process showed a time and concentration depending manner. LLIP showed the poorest cellular uptake which might be due to the presence of high density PEG on the liposome. The PEG on the surface of the liposomes enhanced the hydrophilicity of the liposome and restricted the interaction between the LLIP and the cellular membrane. The FBS contained in the medium could influence on the cellular uptake of each formulation, especially for the cationic liposomes. The fluorescence of the cells treated with CL decreased notable in the presence of 10% FBS, which might be caused by the aggregation of the positively charged CL in the serum.

The BBB model *in vitro* was established to evaluate the transcytosis ability of each formulation. In order to further mimic properties of BBB, we cultured the BCECs on the top side of the membrane of cell culture inserts and the ACs on the bottom side, where the ACs can gain their processes through the membrane pores to contact BCECs. Since more and more evidence illustrated that ACs played an important role in the anatomical formation of BBB and functional expression of its specific properties, this model can be characterized as tight junction and specific functional proteins such as enzymes, transporters. Tight junctions between the BCECs played an important role in maintaining the barrier properties of the BBB *in vitro*. The characterization results of the co-culture showed the TEER values was >250 $\Omega\,cm^2$ of BBB model *in vitro* (Du et al., 2008). The scanning electron microscope and transmission electron microscope displayed the tight junction between two endothelial cells and the astrocytes could spread its foot through the membrane pore to touch the endothelial cells. In the transendothelial ability study on BBB model *in vitro*, for all formulations contacted with the BCECs directly, the cytotoxicity of each formulation might affect the final result. Cytotoxicity result showed that at the amount of 240 nmol for 12 h contact with the BCECs, the cytotoxicity of LIP, LLIP, and TAT-LIP was acceptable. The TEER values also confirmed that the BBB model *in vitro* was intact within 6 h. However, the cytotoxicity of CL was too notable to be ignored, while the TEER values had slightly decrease during 6 h. The BBB model might be broken by the CL. We also found the deposit of the CL in the cell culture inserts. This might be the reason that the accumulated clear volume of CL was still lower than that of the TAT-LIP.

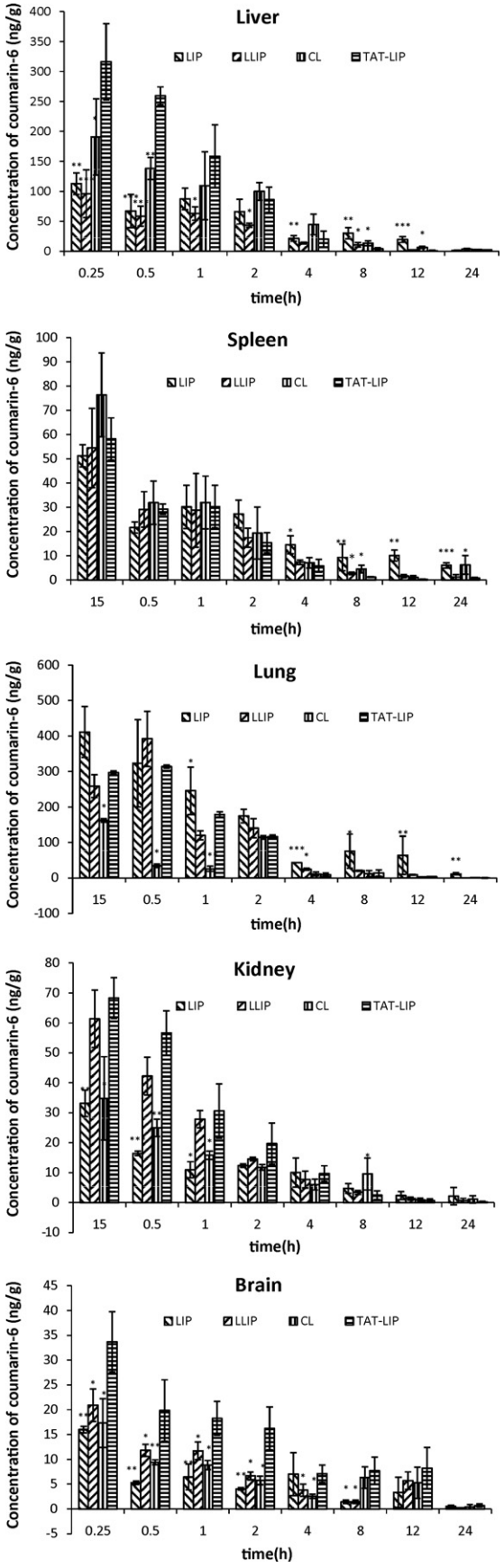

Fig. 11. Biodistribution of liposomes in mice at different time points, expressed as the concentration of coumarin-6 in different tissues. Data represented the mean ± SD ($n = 3$). $^{*}P < 0.05$; $^{**}P < 0.01$; $^{***}P < 0.001$; versus TAT-LIP.

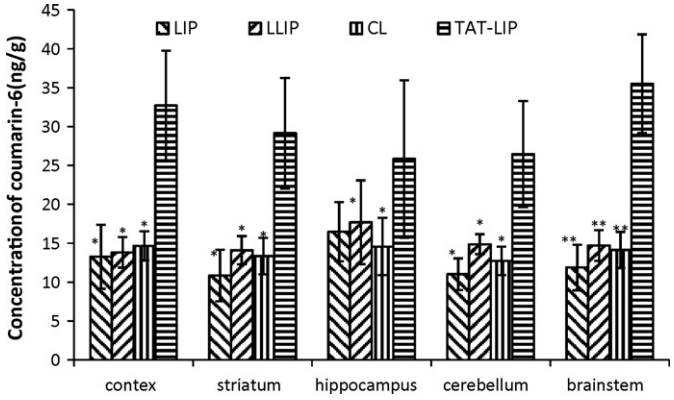

Fig. 12. Biodistribution of liposomes in the brain of rats at different time points, expressed as the concentration of coumarin-6 in different regions of brain. Data represented the mean ± SD ($n = 3$). $^{*}P < 0.05$; $^{**}P < 0.01$; $^{***}P < 0.001$; versus TAT-LIP.

The internalization of TAT-LIP by BCECS was slightly reduced following incubation at 4 °C and in the presence of sodium azide. In contrast to previous reports, this result clearly demonstrates that the uptake of the TAT-LIP was via an energy-dependent process, while the process met the active endocytosis pathway.

To clarify the mechanism by which TAT-LIP was transferred into the cells, BCECs were pretreated with four inhibitors of cellular function: filipin, oxophenylarsine; colchicine, and sucrose; filipin was used to specifically block caveolae-mediated uptake without affecting the function of coated pits (Schnitzer et al., 1994; Orlandi and Fishman, 1998); sucrose is known to inhibit fluid-phase endocytosis; colchicines is to inhibit macropinobytosis; oxophenylarsine is to inhibit clathrin mediated endocytosis. The internalization of TAT-LIP by BCECS was slightly reduced following incubation with oxophenylarsine, colchicine, and sucrose. This active endocytosis might be mediated via multiple pathways, including the clathrin mediated endocytosis and the macropinocytosis.

Both the positive and the negative charge might decrease the cellular uptake of TAT-LIP obviously. That could be inferred that the pathway of TAT-LIP across the BBB might be the absorptive endocytosis. The free TAT did not influence the internalization of TAT-LIP possibly due to its weak positive charge.

The transendothelial transport studies were carried in the presence of heparin, polylysine, and free TAT. All of these substances blocked the transport of the TAT-LIP. This result confirmed that the absorptive endocytosis might be one of the mechanisms of TAT-LIP crossing the BBB. Whether there were other pathways needed further research.

Recently, near-infrared (NIR) fluorescence imaging has emerged as a potential tool for imaging (Ntziachristos et al., 2003; Frangioni, 2003) In the NIR wavelength range of 700–900 nm, light penetrates relatively deep into tissue. The NIR fluorescence imaging offers advantages such as non-radioactivity, high sensitivity compared with conventional techniques (Xu et al., 2007; Tromberg et al., 2008). A near-Infrared dye DIR was enveloped in each liposome. In order to demonstrate the delivery of each formulation into mouse brain, NIR fluorescence imaging experiments were performed. The TAT-LIP showed the highest accumulation in the brain.

The quantitative study of biodistribution could reveal the character of each formulation *in vivo* more precisely and literally. The data had showed that the TAT-LIP accumulated the most in the brain of all within 24 h after the administration. But the concentration of TAT-LIP in the liver and kidney was high within 4 h after the administration. These data showed that though the TAT-LIP could transport into the brain effectively, it also might accumulate

in other tissues. This delivery system could not target to the brain specially. How to enhance the specificity of this delivery system was in study now.

Biodistribution test of mice had showed a great quantity of TAT-LIP was accumulated in the brain one hour after the administration. In order to determine which brain regions took up different formulations more readily, the biodistribution of liposomes in special regions of rat's brain was evaluated quantitatively 1 h after the administration. The concentration of TAT-LIP in each region of the brain was still highest of all. The concentrations of different liposomes in these five regions were almost the same at 1 h after the administration, indicating that all the formulations were distributed in the brain uniformly.

Acknowledgments

This research was supported by the National Basic Research Program (2007CB935801) of China, National Natural and Science Foundation of China (No. 30873166), and the National S & T Major Project of China (No. 2009ZX09310-002).

Appendix A. Supplementary data

Supplementary data associated with this article can be found, in the online version, at doi:10.1016/j.ijpharm.2011.07.021.

References

Banks, W.A., Robinson, S.M., Nath, A., 2005. Permeability of the blood–brain barrier to HIV-1 Tat. Exp. Neurol. 193, 218–227.
Brooks, H., Lebleu, B., Vives, E., 2005. Tat peptide-mediated cellular delivery: back to basics. Adv. Drug Deliv. Rev. 57, 559.
Cardoso, F.L., Brites, D., Brito, M.A., 2010. Looking at the blood–brain barrier: molecular anatomy and possible investigation approaches. Brain Res. Rev. 64, 328–363.
Cecchell, R., Berezowski, V., Lundquis, S., Culot, M., Renfte, M., Dehouck, M.P., Fenart, L., 2007. Modelling of the blood–brain barrier in drug discovery and development. Nat. Rev. Drug Discov. 6, 650–661.
Chen, Y., Dalwadi, G., Benson, H.A.E., 2004. Drug delivery across the blood–brain barrier. Cur. Drug Deliv. 1, 361–376.
Chen, Q., Gong, T., Liu, J., Wang, X., Fu, H., Li, Y., Zhang S Z., 2009. Synthesis, in vitro and in vivo characterization of glycosyl derivatives of ibuprofen as novel prodrugs for brain drug delivery. J. Drug Target. 4, 318–328.
Chen, H., Tang, L., Qin, Y., Yin, Y., Tang, J., Tang, W., Sun, X., Zhang, Z., Liu, J., He, Q., 2010. Lactoferrin-modified procationic liposomes as a novel drug carrier for brain delivery. Eur. J. Pharm. Sci. 40, 94–102.
Chertok, B., David, A.E., Moffat, B.A., Yang, V.C., 2009. Substantiating in vivo magnetic brain tumor targeting of cationic iron oxide nanocarriers via adsorptive surface masking. Biomaterials 30, 6780–6787.
Derossi, D., Calvet, S., Trembleau, A., Brunissen, A., Chassaing, G., Prochiantz, A., 1996. Cell internalization of the third helix of the Antennapedia homeodomain is receptor independent. J. Biol. Chem. 271, 18188–18193.
Du, J., Lu, W.-L., Ying, X., Liu, Y., Du, P., Tian, W., Men, Y., Guo, J., Zhang, Y., Li, R.-J., Zhou, J., Lou, J.-N., Wang, J.-C., Zhang, X., Zhang, Q., 2008. Dual-targeting topotecan liposomes modified with tamoxifen and wheat germ agglutinin significantly improve drug transport across the blood–brain barrier and survival of brain tumor-bearing animals. Mol. Pharm. 6, 905–917.
Fawell, S., et al., 1994. Tat-mediated delivery of heterologous proteins into cells. Proc. Natl. Acad. Sci. U.S.A. 91, 664–668.
Frangioni, J.V., 2003. In vivo near-infrared fluorescence imaging. Curr. Opin. Chem. Biol. 7, 626–634.
Han, H.D., Lee, A., Song, C.K., Hwang, T., Seong, H., Lee, C.O., Shin, B.C., 2006. In vivo distribution and antitumor activity of heparin-stabilized doxorubicin-loaded liposomes. Int. J. Pharm. 313, 181–188.
Hu, K., Li, J., Shen, Y., Lu, W., Gao, X., Zhang, Q., Jiang, X., 2009. Lactoferrin-conjugated PEG–PLA nanoparticles with improved brain delivery: in vitro and in vivo evaluations. J. Control. Release 134, 55–61.
Kaur, I.P., Bhandari, R., Bhandari, S., Kakkar, V., 2008. Potential of solid lipid nanoparticles in brain targeting. J. Control. Release 127, 97–109.
Kheirolomoom, A., Ferrara, K.W., 2007. Cholesterol transport from liposomal delivery vehicles. Biomaterials 28, 4311–4320.
Lasic, D.D., 1996. Doxorubicin in sterically stabilized liposomes. Nature 380, 561–562.
Li, S.-D., Huang, L., 2010. Stealth nanoparticles: high density but sheddable PEG is a key for tumor targeting. J. Control. Release 145, 178–181.
Liu, L., Guo, K., Lu, J., Venkatraman, S.S., Luo, D., Ng, K.C., Ling, E.-A., Moochhala, S., Yang, Y.-Y., 2008. Biologically active core/shell nanoparticles self-assembled from cholesterol-terminated PEG-TAT for drug delivery across the blood–brain barrier. Biomaterials 29, 1509–1517.
Loret, E.P., Vives, E., Ho, P.S., Rochat, H., Van Rietschoten, J., Johnson Jr., W.C., 1991. Activating region of HIV-1 Tat protein: vacuum UV circular dichroism and energy minimization. Biochemistry 30, 6013–6023.
Lu, W., Tan, Y.-Z., Hua, K.-L., Jiang, X.-G., 2005. Cationic albumin conjugated PEGylated nanoparticle with its transcytosis ability and little toxicity against blood–brain barrier. Int. J. Pharm. 295, 247–260.
Miller, C.R., Bondurant, B., Mc Lean, S.D., Mc Govern, K.A., O'Brien, D.F., 1998. Liposome–cell interactions in vitro: effect of liposome surface charge on the binding and endocytosis of conventional and sterically stabilized liposomes. Biochemistry 37, 12875–12883.
Newton, H.B., 2006. Advances in strategies to improve drug delivery to brain tumors. Expert Rev. Ther. 6, 1495–1509.
Ntziachristos, V., Bremer, C., Weissleder, R., 2003. Fluorescence imaging with near infrared light: new technological advances that enable in vivo molecular imaging. Eur. Radiol. 13, 195–208.
Orlandi, P.A., Fishman, P.H., 1998. Filipin-dependent inhibition of cholera toxin evidence for toxin internalization and activation through caveolae-like domains. J. Cell Biol. 141, 905–915.
Pardridge, W.M., 1994. New approaches to drug delivery through the blood–brain barrier. Trends Biotechnol. 12, 239–245.
Pardridge, W.M., 2002. Why is the global CNS pharmaceutical market so underpenetrated? Drug Discov. Today 7, 5–7.
Parr, M.J., Ansell, S.M., Choi, L.S., Cullis, P.R., 1994. Factors influencing the retention and chemical stability of poly(ethylene glycol)–lipid conjugates incorporated into large unilamellar vesicles. Biochim. Biophys. Acta 1195, 21–30.
Pham, W., Zhao, B.-Q., Lo, E.H., Medarova, Z., Rosen, B., Moore, A., 2005. Crossing the blood–brain barrier: a potential application of myristoylated polyarginine for in vivo neuroimaging. Neuroimage 28, 287–292.
Qin, Y., Fan, W., Chen, H., Yao, N., Tang, W., Tang, J., Yuan, W., Kuai, R., Zhang, Z., Wu, Y., He, Q., 2010. In vitro and in vivo investigation of glucose-mediated brain-targeting liposomes. J. Drug Target. 18, 536–549.
Santra, S., Yang, H., Stanley, J.T., Holloway, P.H., Moudgil, B.M., Walter, G., 2005. Rapid and effective labeling of brain tissue using TAT-conjugated CdS:Mn/ZnS quantum dots. Chem. Commun. 25, 3144–3146.
Schnitzer, J.E., Oh, P., Pinney, E., Allard, J., 1994. Filipin-sensitive caveolae mediated transport in endothelium reduced transcytosis, scavenger endocytosis and capillary permeability of select macromolecule. J. Cell Biol. 127, 1217–1232.
Schwarze, S.R., et al., 1999. In vivo protein transduction: delivery of a biologically active protein into the mouse. Science 285, 1569–1572.
Siflinger-Birnboim, A., Del Becchio, P.J., Cooper, J.A., Blumenstock, F.A., Shepard, J.N., Malik, A.B., 1987. Molecular sieving characteristics of the cultured endothelial monolayer. J. Cell. Physiol. 132, 111–117.
Temsamani, J., Scherrmann, J.M., 2003. Peptide vectors as drug carriers. Prog. Drug Res. 61, 221–238.
Temsamani, J., Vidal, P., 2004. The use of cell-penetrating peptides for drug delivery. Drug Discov. Today 9, 1012–1019.
Tromberg, B.J., Pogue, B.W., Paulsen, K.D., Yodh, A.G., Boas, D.A., Cerussi, A.E., 2008. Assessing the future of diffuse optical imaging technologies for breast cancer management. Med. Phys. 35, 2443–2451.
Vivès, E., Brodin, P., Lebleu, B., 1997. A truncated HIV-1 Tat protein basic domain rapidly translocates through the plasma membrane and accumulates in the cell nucleus. J. Biol. Chem. 272, 16010–16017.
Wadia, J.S., Dowdy, S.F., 2002. Protein transduction technology. Curr. Opin. Biotechnol. 13, 52–56.
William, M., Pardridge, T., 2005. Drug and gene targeting to the brain via blood–brain barrier receptor-mediated transport systems. Int. Congr. Ser. 1277, 49–62.
Xu, R.X., Young, D.C., Mao, J.J., Povoski, S.P., 2007. A prospective pilot clinical trial evaluating the utility of a dynamic near-infrared imaging device for characterizing suspicious breast lesions. Breast Cancer Res. 9, R88.
Zhao, M., Weissleder, R., 2004. Intracellular cargo delivery using Tat peptide and derivatives. Med. Res. Rev. 24, 1–12.
Zhao, X.B., Muthusamy, N., Byrd, J.C., Lee, R.J., 2007. Cholesterol as a bilayer anchor for PEGylation and targeting ligand in folate-receptor-targeted liposomes. J. Pharm. Sci. 96, 2424–2439.